Characterization of a de novo Designed Heme Protein by EPR and ENDOR Spectroscopy

M. Fahnenschmidt,[a] H. K. Rau,[b] R. Bittl,[a] W. Haehnel,[b] and W. Lubitz*[a]

Abstract: The binding situation of heme incorporated into a de novo synthesized protein is investigated with EPR and ENDOR spectroscopy. The protein was modeled on the cytochrome *b* subunit of the cytochrome bc_1 complex and contains two bis-histidine heme binding sites. The EPR spectra show Fe^{3+} low-spin signals with *g* tensor principal values of 2.97, 2.27, and 1.51 and a contribution of a highly anisotropic low-spin (HALS) species with a g_{max} signal at $g = 3.5$. The regular Fe^{3+} low-spin EPR spectra were simulated based on a *g* strain linewidth-broadening mechanism. The resulting *g* tensor principal values were used for a ligand-field analysis. The ligand-field parameters are typical for bis-histidine ligated hemes with approximately parallel histidine planes. The HALS species is characteristic of bis-histidine ligation with tilted or twisted imidazole planes. The occurrence of both types of heme in the de novo synthesized protein is discussed. The EPR data are supplemented by pulsed ENDOR studies of this protein and are compared with those of metmyoglobin–imidazole and bis-imidazole ferric heme model systems. ENDOR resonances of nitrogen and protons of histidine were identified and used as structural probes for the axial ligation of the hemes.

Keywords: ENDOR spectroscopy · EPR spectroscopy · helical structures · heme proteins

Introduction

De novo design of proteins is a new field that has provided several strategies to approach synthetic proteins with a variety of functions including catalysis and electron transfer. Various de novo synthesized metalloproteins have been obtained with cofactors like heme,[1–5] other metalloporphyrins,[6] iron–sulfur clusters,[7, 8] and mononuclear metal sites.[9–11] Synthetic proteins with heme as the prosthetic group are of particular interest as a result of the wide range of biological functions achieved by natural heme proteins, including oxygen transport and storage (hemoglobin, myoglobin), electron transfer (cytochromes), and catalysis (catalases, peroxidases).[12] The versatility in function of the heme group arises in particular from the diversity of axial ligation and other interactions with the surrounding protein. Here, we focus on properties of cytochrome *b* which constitutes the heart of the cytochrome bc_1 and the cytochrome b_6f complexes in mitochondria and chloroplasts, respectively.

[a] M. Fahnenschmidt, Dr. R. Bittl, Prof. Dr. W. Lubitz
Technische Universität Berlin
Max-Volmer Institut für Biophysikalische und Physikalische Chemie
Strasse des 17. Juni 135, D-10623 Berlin (Germany)
Fax: (+49) 30-3142-1122
E-mail: lubitz@echo.chem.tu-berlin.de

[b] Dr. H. K. Rau, Prof. Dr. W. Haehnel
Albert-Ludwigs-Universität Freiburg
Institut für Biologie II/Biochemie
Schänzlestrasse 1, D-79104 Freiburg (Germany)

Choma et al.[1] were the first to synthesize a four-helix-bundle with a single heme. Robertson et al.[2] constructed multi-heme proteins. These systems have been termed maquettes. The maquettes are formed from an amphiphilic helix; this is dimerized by a disulfide bridge between N-terminal cysteines and assembled into a bundle of four helices with parallel orientation.[2] This design concept has recently been extended by synthesis of peptides forming a helix–loop–helix structure to allow alternative four-helix-bundle topologies.[13] The assembly of the amphiphilic helices is driven to a great extent by the formation of a hydrophobic core of the bundle. However, the association of single helices or helix–turn–helix peptides includes several possibilities of the interfacial packing[14] which are difficult to predict. The modular design strategy of a template-assembled synthetic protein (TASP) introduced by Mutter et al.[15] solves this protein-folding problem. It provides flexibility in protein design with respect to position and orientation of the helices by their coupling to a cyclic decapeptide template. The modular synthesis of a TASP has been combined with the incorporation of redox-active cofactors to build a four-helix-bundle protein accomodating two bis-histidine ligated heme groups.[16, 17] By following the structure of cytochrome *b*[18, 19] we have attached to the template two parallel heme binding helices with two alternating antiparallel helices, which shield the two hydrophobic heme binding sites from the hydrophilic exterior. This synthetic heme protein assembled from purified polypeptide building blocks is termed MOP for modular protein.

  0947-6539/99/0508-2327 $ 17.50+.50/0

In this contribution we determine the properties of the heme groups in the synthetic protein, investigate the type of the axial ligands, their distance from the metal center, and the orientation relative to each other. This detailed analysis is performed by EPR and ENDOR spectroscopy with the oxidized heme as a paramagnetic probe.

The Fe^{3+} central ion of the heme can adopt two spin states:[20] a high-spin state ($S = 5/2$) with an axial g tensor ($g_{\parallel} = 2$ and $g_{\perp} = 6$) and a low-spin state ($S = 1/2$) with a rhombic g tensor. The principal g values for the $S = 1/2$ state depend critically on the type and arrangement of the axial ligands of the heme. The detection of the spin state in the EPR spectrum and the evaluation of the g tensor values in terms of a ligand-field analysis[21] is the basis for investigating the coordination sphere of the heme group in the protein.

EPR spectroscopy has been used[1, 2, 5, 22] to characterize the heme incorporation in maquettes. Here we extend this approach and additionally use ENDOR spectroscopy to study the heme and its binding site in the de novo synthesized protein. ENDOR reveals the hyperfine interactions of protons and ^{14}N nuclei in the environment of the Fe^{3+} of the heme group.[23] The ENDOR measurements on the de novo synthesized protein will be compared with those of the natural heme protein derivative, metmyoglobin with an additional imidazole ligand (MbIm), and the model complex bis-imidazole ferric heme ($PPIX(Fe)Im_2$).

Results and Discussion

Design concept: The design of both four-helix-bundle proteins, maquette[2] and MOP,[16] is based on the stabilization of the molecule by the assembly of the amphiphilic helices, which form a hydrophobic interior, and by the ligation of each heme group with two histidines. The helices are additionally stabilized by salt bridges. This is achieved by glutamate and lysine being held apart by four residues. The concept of assembly and topology of the maquette and the MOP is, however, significantly different. The dimerization of the single helices through the N-terminal cysteines after oxidation by air and the self-assembly of these dimers to the maquette are accomplished within a short time. In contrast, the synthesis of the MOP includes many additional steps of purification, chemical modification, and selective ligation to the template. Figure 1 shows a schematic drawing of the MOP.

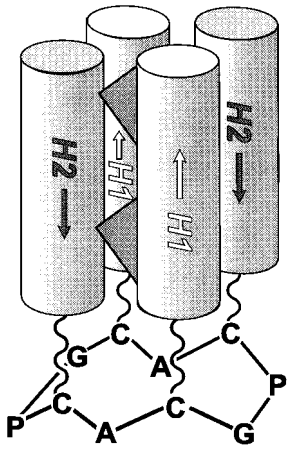

Figure 1. Schematic representation of the modular protein (MOP). The design concept is based on the modular strategy of a template-assembled synthetic protein.[17] The fixation of helices (shown as columns) on a template allows control of antiparallel orientation and the desired arrangement of helices. The MOP shown here contains two different helices (H1 and H2) and two heme binding sites. The two hemes are indicated by squares (for details see text).

It includes essential features of the heme-binding core formed by the four transmembrane helices A, B, C, and D of the cytochrome b subunit in the cytochrome bc_1 complex.[19, 24] The residues in the center of the four transmembrane helices and in particular those presumably in contact with the heme groups were conserved in the design. The other residues oriented towards the exterior of the bundle were changed to hydrophilic and helix-stabilizing residues.[16, 17] The amino acid sequences of the helical peptides H1 and H2 with a bromoacetyl group at the N-terminus (H1) and at the ε-amino group of the C-terminal lysine (H2) are:

Br-H1: BrAc–GGELREL**H**EKLAKQ**F**EQLVKL**H**EERAKKL–NH_2
Br-H2: Ac–LEEL**W**KK**G**EELAKKLQEALEK**G**KKLAK(AcBr)–NH_2

The template *cyclo*(CACPGCACPG) and the complete MOP with the helices H1 and H2 bound by thioether linkages to the cysteine residues of the cyclic decapeptide template are depicted in Figure 1.

Helix H1 contains two histidines separated by 13 residues as found in the heme-binding helices B and D of the natural protein. Furthermore, a phenylalanine is introduced in the center of helix H1 as found in helix B of cytochrome *b*. The

Abstract in German: *Die Bindungssituation des in ein de novo synthetisiertes Protein eingebauten Häms wird mit EPR- und ENDOR-Spektroskopie untersucht. Das de novo synthetisierte Protein wurde auf der Basis der Cytochrom b-Untereinheit des bc_1 Komplexes modelliert und enthält zwei Bis(histidin)-Bindungstaschen. Die EPR Spektren des Proteins zeigen Low-spin-Signale des Fe^{3+} mit g-Tensorhauptwerten von 2.97, 2.27 und 1.51 und eine stark anisotrope Low-spin-Spezies (HALS) mit einem Signal bei $g_{max} = 3.5$. Die normalen Low-spin-EPR-Spektren wurden mit einem g-strain-Mechanismus zur Linienverbreiterung simuliert. Die hieraus resultierenden g-Tensorhauptwerte bilden die Grundlage für eine Ligandenfeldanalyse. Die erhaltenen Ligandenfeldparameter sind typisch für durch zwei Histidine gebundenes Hämin mit annähernd parallelen Histidinebenen. Die HALS-Spezies ist dagegen charakteristisch für eine Bindung mit verdrehten oder verkippten Histidinebenen. Das Auftreten beider Spezies im de novo synthetisierten Protein wird diskutiert. Die EPR-Daten werden durch Puls-ENDOR-Studien an diesem Protein ergänzt, welche mit denen von Modellsystemen, Metmyoglobin–Imidazol und Hämin–Bis(imidazol), verglichen werden. ENDOR-Resonanzen von Stickstoff und Protonen des Histidins wurden identifiziert und als strukturelle Sonden für die axiale Bindung der Hämine eingesetzt.*

  0947-6539/99/0508-2328 $ 17.50+.50/0 *Chem. Eur. J.* **1999**, *5*, No. 8

termini of the helices have been blocked either by acetyl or amide to reduce the helix dipole for additional stabilization. The arginines spaced by three residues from the heme-ligating histidines should compensate for the negative charges of the propionate groups of the heme. Helix H2 is bound to the template in antiparallel orientation to helix H1. Helix H2 was modeled after the natural helices A and C, and contains two conserved glycines which are positioned at the same height as the two histidines in H1 and a conserved tryptophan. The linkage of the helices to the template and the branched structure of the MOP favors the formation of the helix bundle by a small change in entropy between the unfolded and folded state compared with the assembly of independent substructures.[25]

The design of the MOP[17] is essentially different from that of the maquette.[2] The latter is a homotetramer of a single helix with four hemes and has four charged N- and C-termini, while the MOP is synthesized from two different helices with blocked termini in parallel orientation and binds two hemes. An advantage of the modular synthesis of the MOP is the possibility of controlling the orientation and position of the helices bound to the template. However, the fixation on the peptide template may restrict the freedom in the geometric arrangement of the helices. As recently shown,[26] this problem may be avoided by suitable linkers.

EPR spectroscopy: The EPR spectra of MOP and MbIm are shown in Figure 2. The signals at g values of 3.0, 2.3, and 1.5 are characteristic for low-spin Fe^{3+}. The spectrum of the MOP shows an additional shoulder at $g = 3.5$. The signal at $g = 6$ is diagnostic for the $g_\perp$ component of high-spin Fe^{3+},[20] the respective $g_\parallel = 2$ signal is superimposed on other signals at $g = 2$. The very small signal at $g = 4.3$, assigned to rhombic Fe^{3+},[27] and the signal at $g = 2$ can be attributed to a small amount of paramagnetic impurities in the buffer.

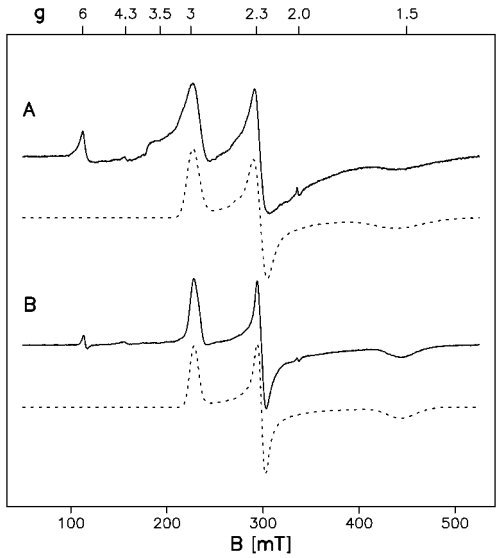

Figure 2. X-band EPR spectra of MOP (**A**) and MbIm (**B**). The simulations of the Fe^{3+} low-spin spectra are shown as dotted lines. The extracted g values are collected in Table 1. Experimental conditions: $T =$ 20 K, 9.44 GHz microwave frequency, 5 mW microwave power, 100 kHz modulation frequency, 1 mT modulation amplitude, 15 min total recording time for each spectrum. The simulation is based on a special case in the g strain theory of Hagen et al.,[36] where the g tensor principal values are treated as statistical variables. The linewidth is determined by the standard deviations σ_1, σ_2, σ_3 of the g tensor values. For the MOP we obtained $\sigma_1 = 0.07$, $\sigma_2 = 0.03$, $\sigma_3 = 0.08$, and correlation coefficients $r_{12} = -0.95$, $r_{23} = -0.95$, and $r_{13} = 0.95$. For MbIm $\sigma_1 = 0.05$, $\sigma_2 = 0.02$, $\sigma_3 = 0.04$, and $r_{12} = -0.95$, $r_{23} = -0.95$, $r_{13} = 0.95$. For the respective g values see Table 1.

The EPR spectrum of the MOP in Figure 2A indicates predominance of low-spin and only a little high-spin heme. The detection of the low-spin state provides clear evidence for a specific heme incorporation through strong axial coordination by two histidine ligands. The high-spin state occurs when only weak axial ligands are provided as in samples of free heme in aqueous solution,[28] or when only one histidine ligand is bound to heme as in aqueous metmyoglobin.[29] If a second imidazole ligand is added to metmyoglobin, imidazole is bound to the distal site of the heme as a sixth ligand[30] and a conversion to the low-spin state occurs,[31] as can be seen in the EPR spectrum of MbIm in Figure 2B. For a quantitative comparison of the spin states in the EPR spectrum of the MOP it should be noted that the signal of high-spin ($S = 5/2$) heme at $g_\perp = 6$ tends to dominate the EPR spectrum as a result of the large transition moment even when the concentration of high-spin Fe^{3+} is considerably lower than that of low-spin Fe^{3+} ($S = 1/2$).[32] An estimation based on the simulation of the spectra yields a ratio of about 1:100 for the ratio of the high- to low-spin heme form in the MOP, without accounting for the shoulder at $g \sim 3.5$. Thus, the amount of high-spin heme is almost negligible.

In the following we will inspect the low-spin Fe^{3+} EPR spectra of the MOP with MbIm as reference to extract further details of the heme binding situation. The linewidths of the MOP and MbIm are in the order of several 100 MHz, thereby ruling out relaxation, protein dynamics, or unresolved hyperfine splittings as origin of the line broadening. It has been shown[33, 34] that the dominant line-broadening mechanism in EPR spectra of low-spin heme proteins is g strain. This is caused by structural microheterogeneities in the environment of the paramagnetic center.[35] We simulated the spectra of the Fe^{3+} low-spin species in Figure 2 based on the g strain line-broadening model of Hagen et al.[36] The parameters for the simulations shown in Figure 2 are given in the figure caption. The linewidth of the low-spin EPR spectrum of the MOP is larger than that of the MbIm. This increased linewidth is interpreted as a larger g strain; this indicates a higher degree of microheterogeneity in the MOP. The principal g tensor values obtained from the simulation are given in Table 1. In a maquette with four hemes a similar EPR spectrum of a low-spin Fe^{3+} species was found[22] with g tensor values $g_1 = 2.89$, $g_2 = 2.24$, and $g_3 = 1.54$.[2]

In natural heme proteins with bis-histidine binding pockets g tensor values comparable to those found in the de novo synthesized heme proteins were observed. For example, cytochrome b_5 shows g tensor values of 3.03, 2.24, and 1.46.[37] In this protein the histidine planes are oriented parallel to each other.[38] A correlation between the orientation of the histidine ligand planes and the g tensor values was established on the basis of ligand-field theory.[39] The measured g tensor values collected in Table 1 suggest that the

Table 1. EPR data for the MOP and MbIm.

	MOP	MbIm
g_1[a]	2.97 (±0.01)	2.96 (±0.01)
g_2	2.27 (±0.01)	2.26 (±0.01)
g_3	1.51 (±0.02)	1.51 (±0.02)
V/λ[b]	1.84 (±0.03)	1.85 (±0.03)
Δ/λ	3.30 (±0.13)	3.32 (±0.13)
V/Δ	0.56 (±0.02)	0.56 (±0.02)

[a] The error in the g tensor values was calculated based on an accuracy of 1 mT for the magnetic field (5 mT for g_3) and 10 MHz for the microwave frequency. The g tensor values obtained from the frozen powder spectrum of MbIm are somewhat different from those found in single crystals of MbIm for which $g_z = 2.91$, $g_y = 2.26$, and $g_x = 1.53$ were measured.[31] [b] The ligand-field parameters of MbIm and MOP were obtained from a ligand-field analysis of the g tensor principal values.[21] The rhombic splitting V and the tetragonal splitting Δ were determined in units of the spin-orbit coupling constant λ.

histidine planes in our de novo synthesized protein are also oriented parallel to each other.

In the following we will perform a ligand-field analysis of the g tensor values summarized in Table 1 to obtain more detailed information on the electronic structure and the coordination geometry in our de novo synthesized protein. For low-spin Fe^{3+} complexes this analysis yields the relative energies of the three lowest occupied d orbitals depicted in Figure 3.[21] The difference between the ligand-field strengths

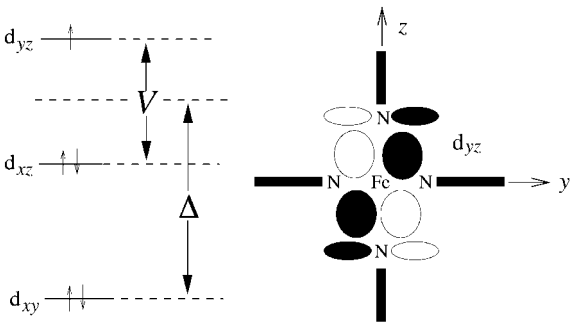

Figure 3. Left: Splitting of the three lowest occupied d orbitals in low-spin Fe^{3+} complexes: d_{xy} is separated from d_{xz} and d_{yz} by the tetragonal splitting parameter Δ, and d_{xz} and d_{yz} are separated by the rhombic splitting parameter V. Right: Schematic picture showing the orientation of the partially filled d_{yz} orbital of the iron, the porphyrin plane and the 2 imidazole ligands for a centrosymmetric bis-imidazole ferric porphyrin system. In this idealized complex g_z is perpendicular to the porphyrin plane, g_y and g_x lie in the porphyrin plane. Both imidazole planes eclipse the Fe–N bonds of the porphyrin in the g_x direction.

of the axial ligands and the porphyrin ligand causes the d_{xy} orbital, lying in the porphyrin plane, to be separated from the orbitals d_{xz} and d_{yz} by the tetragonal splitting Δ. The d_{xz} and the d_{yz} orbital are also energetically different (rhombic splitting V). Taylor's method of ligand-field analysis[21] yields a simple relation between the g tensor values and the ligand-field parameters V and Δ in units of the spin–orbit coupling constant λ; see Equations (1) and (2).

$$\frac{V}{\lambda} = \frac{g_x}{g_z + g_y} + \frac{g_y}{g_z - g_x} \quad (1)$$

$$\frac{\Delta}{\lambda} = \frac{g_x}{g_z + g_y} + \frac{g_z}{g_y - g_x} - \frac{1V}{2\lambda} \quad (2)$$

We assigned the g tensor values g_1, g_2, and g_3 obtained from the simulations of the EPR spectra in Figure 2 to g_z, g_y, and g_x, respectively. This assignment is based on single-crystal EPR measurements of other low-spin heme proteins[31, 40] and model compounds.[41] These measurements showed unambiguously that the principal axis for the largest g value assigned to g_z is approximately parallel to the heme normal. However, discrepancies exist for low-spin metmyoglobin derivatives in the reported directions for g_x (assigned to the smallest g value) and g_y.[42, 43] In the following discussion we adapted a schematic representation (see Figure 3) of a centrosymmetric bis-imidazole ferric porphyrin system with the orientation of the g tensor axis from Soltis and Strouse[41] and Quinn et al.[44]

The results of the ligand-field analysis are summarized in Table 1. We determined the tetragonality Δ/λ, the rhombicity V/Δ, and the relative rhombic splitting V/λ for MOP and MbIm. The values obtained for the MOP and MbIm are very similar. The tetragonality Δ/λ is a measure of the axial ligand donor strength. The rhombicity V/Δ describes the geometric distortion of the complex. According to the work of Peisach et al.[28] the values Δ/λ and V/Δ determined for MOP and MbIm are typical for bis-histidine ligated hemes. The rhombic splitting V gives further indication on the relative orientation of the histidine planes. The rhombic splitting V is mainly caused by a π ligand-to-metal bonding interaction of an axial ligand orbital with the iron d_{yz} orbital, which raises the energy of d_{yz}. The interaction is schematically depicted in Figure 3 (right). Alternatively, π metal-to-ligand back-bonding could lower the energy of the d_{xz} orbital. This second possibility is favored in the work of Scholes et al.,[45] but would require an exchange of the directions of the g_x and g_y axes in Figure 3. Regardless of which interaction dominates, the rhombic splitting V is very sensitive to changes in the geometrical arrangement of the axial ligands. For a parallel orientation of the histidine planes the rhombic splitting V should reach a maximum value of 2λ.[39] The large value of V/λ obtained for the MOP and MbIm shows an almost perfect parallel orientation of the histidine planes in these compounds. When the two histidine planes approach a perpendicular orientation, the net effect of the different interactions of the π system of the axial histidines with the d_{xz} and d_{yz} orbitals cancels[46] and V becomes smaller.

For small V, ligand-field analysis yields g_z values as high as 3.8.[39, 47] Ferric protohemin model complexes with sterically hindered imidazole derivatives actually yield EPR spectra with pronounced signals at g_{max} considerably larger than $g = 3.0$ and a broad tail, which extends below $g \sim 1.0$.[32, 39, 48] These compounds are often termed HALS (highly anisotropic low-spin) systems.[48, 49] We suggest that the shoulder in the EPR spectrum of the MOP at $g = 3.5$ (Figure 3) is a result of a contribution of a HALS species with twisted or tilted histidine planes. The shoulder at $g = 3.5$ is thus assigned to the g_{max} signal of the HALS species. EPR spectra of HALS systems typically extend over a large field range, and the other g tensor components are difficult to detect. In the EPR spectrum of the MOP they are probably obscured by the signals from the regular Fe^{3+} low-spin species. We presume that the relative amount of the HALS system compared with the other Fe^{3+} low-spin species is rather large, since the EPR intensity of the

0947-6539/99/0508-2330 $ 17.50+.50/0 *Chem. Eur. J.* **1999**, *5*, No. 8

HALS is spread out over a wide field range. Mössbauer studies of a MOP sample with ^{57}Fe enriched hemes lead to the conclusion that the HALS system with twisted or tilted histidine planes might contribute to about 50% of the sample.[50] In the EPR spectrum of a maquette containing four heme groups[22] a shoulder at $g \sim 3.5$ is also visible. It should be noted that the EPR spectra of the natural heme protein (cytochrome *b*) also show signals typical for HALS systems from the two b-type heme groups. The g_{max} value is 3.78 for the low-potential and 3.45 for the high-potential heme.[47, 51] In the structure of cytochrome *b* in the cytochrome bc_1 complex[52] the heme-ligating histidines appear to be oriented perpendicular to each other at the low-potential heme and rather tilted at the high-potential heme.

For our MOP two different midpoint potentials have been determined by redox titrations (-106 and -170 mV).[17] This was recently supported by electrochemical measurements of the MOP coupled to a gold surface.[53] The higher redox potential was found for the heme group next to the template.[53] It is tempting to speculate that in the MOP the two different redox potentials and EPR spectroscopic properties might be correlated. However, on the basis of our present EPR data it is impossible to assign the two different species (HALS and regular low-spin Fe^{3+}) specifically to the two heme binding pockets of the MOP.

ENDOR spectroscopy: To obtain more detailed information on the binding situation of the hemes in the MOP we have applied ENDOR spectroscopy (for reviews see e.g. Hoffman et al.[54] and Hüttermann[55]). In ENDOR spectra of proteins with histidine ligated heme resonances of ^{14}N and ^{1}H nuclei can be observed,[45] which appear in different spectral ranges because of the large difference in the magnetic moments. ^{14}N and ^{1}H nuclei are both part of the heme cofactor and the axial histidine ligands. Here our main interest is the identification of the ENDOR resonances of the axial histidine ligands to characterize the heme incorporation in the de novo synthesized protein.

Scholes et al.[45] have shown that the ^{14}N ENDOR resonances of the ligated imidazoles are superimposed on those of the heme moiety. These authors were able to identify by ^{15}N labeling only one peak from the imidazole ligand in ^{14}N cw-ENDOR of MbIm. We also observed this imidazole ^{14}N peak in our ENDOR spectra of MbIm and MOP (data not shown), thus corroborating the binding of the heme by histidine in the MOP. No further information on the axial coordination of the heme was obtained as a result of problems of spectral resolution in the ^{14}N ENDOR range. In the following we will therefore focus on ^{1}H ENDOR, in particular on the resonances of the ring protons of the axial histidine ligands.

To assign the ^{1}H ENDOR resonances in the MOP we compare the pulsed ENDOR spectra obtained with those of heme model complexes. For this purpose we chose bis-imidazole ferric heme (PPIX(Fe)Im_2) and MbIm. Furthermore, the pulsed ENDOR spectra in this work will be related to cw-ENDOR spectra of bis-imidazole ferric tetraphenylporphyrin (TPP(Fe)Im_2),[45] for which a detailed analysis is available.

The ENDOR spectra of the model complex PPIX(Fe)Im_2 recorded at $g_y = 2.3$ prepared with protonated and deuterated imidazole are shown in Figure 4A and 4B, respectively. The ^{1}H ENDOR resonances with splittings larger than 2 MHz, labeled a/a′, b/b′, and c/c′ in the spectrum with protonated imidazole (Figure 4A), are absent in the spectrum with deuterated imidazole (Figure 4B). Thus, these resonances can safely be assigned to the imidazole protons. The hyperfine (hf) splittings are 2.6 MHz (a/a′), 3.2 MHz (b/b′), and 5.2 MHz (c/c′).[56]

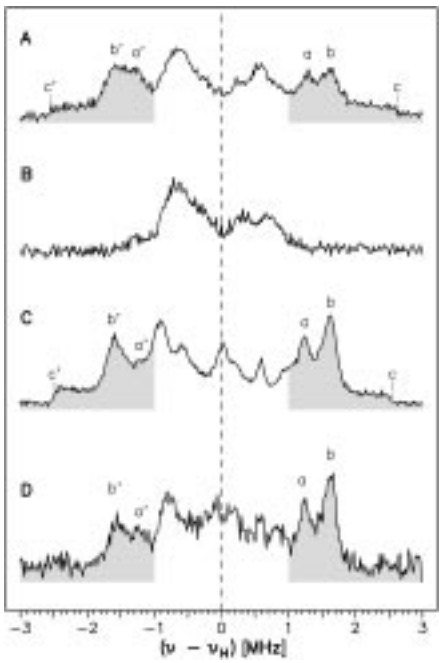

Figure 4. Pulsed ENDOR spectra of PPIX(Fe)Im_2 with protonated (**A**) and deuterated (**B**) imidazole, MbIm (**C**), and MOP (**D**). The shaded areas in the spectra indicate the lines assigned to the imidazole protons H2 and H5. The number of scans for the ENDOR spectra are 25 (**A**), 40 (**B**), 800 (**C**), and 400 (**D**). The spectra of PPIX(Fe)Im_2 were obtained at $g = 2.27$, close to the g_y field position. The Larmor frequency of the protons is $\nu_H = 12.98$ MHz. The spectra of MbIm (**C**) and MOP (**D**) were obtained at $g = 2.28$, close to the g_y field position; $\nu_H = 12.94$ MHz. Within experimental error the peaks (a/a′, b/b′, c/c′) are symmetrically displaced around ν_H. The obtained hf splittings are a/a′: 2.6 MHz (PPIX(Fe)Im_2), 2.5 MHz (MbIm), 2.4 MHz (MOP), b/b′: 3.2 MHz (PPIX(Fe)Im_2), 3.2 MHz (MbIm), 3.2 MHz (MOP), c/c′: 5.2 MHz (PPIX(Fe)Im_2), 5.0 MHz (MbIm), 5.3 MHz (MOP). Experimental errors are ± 0.1 MHz (**C**) and ± 0.2 MHz (**A**, **B**, **D**). The low signal-to-noise ratio in spectrum (**D**) is caused by the significantly smaller concentration of the MOP sample.

X-ray structures of heme model complexes[58, 59] show that the heme *meso* protons are localized at a distance of 4.5 Å, the imidazole protons H3 and H4 at 5.2 Å, and the imidazole protons H2 and H5 at 3.2 Å from the Fe^{3+} (see Figure 5).[60] The largest dipolar interaction is expected for the latter two protons. Therefore, the lines a/a′, b/b′, and c/c′ can be assigned to H2 and H5. The small hf splittings (< 2 MHz) are assigned to the heme moiety and to H3 and H4 of the imidazole[45] and will not be further discussed here. Scholes et al.[45] were able to assign the ^{1}H ENDOR resonances to specific protons on the imidazole ligands by using selectively deuterated imidazole with TPP(Fe)Im_2. We have recorded pulsed ENDOR spectra

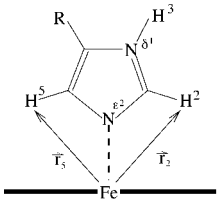

Figure 5. Schematic picture of imidazole (R = H_4) or histidine (R = CH_2–peptide) coordinated to heme.

of PPIX(Fe)Im_2 at the same field position ($g = 2.48$) as in ref. [45] and obtained virtually identical hf splittings. Based on this comparison we assign the ^{1}H ENDOR resonances a/a′ and c/c′ to the imidazole proton H5 and the ENDOR resonances b/b′ to H2. A second line pair for H2 is missing in the ENDOR spectra.

In Figure 4C the ^{1}H ENDOR spectrum of MbIm recorded at $g_y = 2.3$ is shown. In this spectrum, the ENDOR intensities are nonsymmetric with respect to the proton Larmor frequency, and a smaller linewidth and a better resolution than for PPIX(Fe)Im_2 are obtained. The pronounced lines belonging to hf splittings larger than 2 MHz labeled a/a′, b/b′, and c/c′ are typical for the protons H2 and H5 of axial imidazole ligands as discussed above. The hf splittings are 2.5 MHz (a/a′), 3.2 MHz (b,b′), and 5.0 MHz (c/c′). For MbIm prepared with deuterated imidazole the intensity of the ENDOR peaks labeled a/a′, b/b′ and c/c′ decreases whereas the peak positions remain unchanged (data not shown). The remaining lines a/a′, b/b′, c/c′ must belong to the proximal histidine of myoglobin. This shows that this histidine and the added imidazole ligand have the same hyperfine couplings within experimental error and thus a very similar coordination geometry.

In Figure 4D the ENDOR spectrum of the MOP recorded at $g_y = 2.3$ is shown. This spectrum is almost identical to that of MbIm in Figure 4C. However, in the EPR spectrum of the MOP a considerable contribution of a HALS species was detected in contrast to MbIm. Obviously, no ENDOR response is obtained from the HALS species, probably as a result of a different relaxation behavior of the HALS and regular low-spin Fe^{3+} species. In the spectral region with splittings larger than 2 MHz two line pairs labeled a/a′ and b/b′ were observed. Unfortunately, the low signal-to-noise ratio did not allow a clear detection of the expected line pair c/c′. The hf splittings are 2.4 MHz (a/a′) and 3.2 MHz (b/b′). Within experimental error the hf splittings corresponding to the imidazole protons H2 and H5 of PPIX(Fe)Im_2, MbIm, and MOP are identical. The identification of the ENDOR resonances of these protons in the de novo synthesized protein confirms the binding of the low-spin heme by axial histidine residues. The detection of *both* protons, H2 (b/b′) and H5 (a/a′), further indicates that the heme is coordinated by the N(ε^2) atom of the histidine ligand (the two nitrogen atoms of the histidine side chain are labeled δ^1 and ε^2 with ε^2 coordinated to the heme iron[67]). If the ligation were through the N(δ^1) atom of the histidine one would expect hf splittings larger than 2 MHz from only one neighboring proton (H2) (see Figure 5).

The protons H5 and H2 show different hf splittings (a/a′ and b/b′, respectively) in all investigated systems. This could be a result of a difference in the dipolar or the isotropic hyperfine coupling. For a symmetric binding situation as depicted in Figure 5 ($r_2 = r_5$) the same dipolar interaction for protons H2 and H5 is expected. X-ray structures of model systems[39, 44, 58] show almost identical distances between the iron and H2, and the iron and H5. The clear difference in the respective hyperfine splittings can, therefore, only be explained as a difference in the isotropic hyperfine coupling. Indeed, NMR measurements on low-spin heme proteins and model compounds yielded considerable larger contact shifts for H2 than for H5.[61–65] It can be assumed that for the systems studied in this paper (PPIX(Fe)Im_2, MbIm, MOP) with imidazole or histidine ligation a similar situation is present.

In MbIm the histidine ligation is known to be symmetric; distances from the iron to H2 and to H5 lie in the range of 3.2 – 3.3 Å. The spectrum of our MOP is very similar with respect to line position, relative intensities, and linewidths to that of MbIm. We therefore conclude that the two histidines in the MOP are bound to the Fe^{3+} in a very similar way with an Fe–N(ε^2) distance of approximately 2.0 Å as found for the histidine in myoglobin.[30]

Conclusion

In this work we investigated a de novo synthesized protein (MOP) by EPR and ENDOR techniques with the incorporated heme as paramagnetic probe. Comparison with a natural heme protein derivative, metmyoglobin – imidazole (MbIm), showed that the EPR spectra of both proteins are dominated by low-spin Fe^{3+} signals. A ligand-field analysis of the corresponding g tensor values demonstrated that this state is caused by strong ligation of two histidine residues with approximately parallel planes. A linewidth analysis indicated a somewhat higher structural disorder in case of the MOP, which may be caused by the fixation of the helical peptide chains on a template. ENDOR spectroscopy on MOP and MbIm was used to identify protons and the coordinating nitrogen from the axially bound histidine and imidazole ligands. Comparison with earlier model studies[45] clearly showed that the coordination geometry is very similar in both systems. The distance between the Fe^{3+} and N(ε^2)(Im) is approximately 2.0 Å and the ligands are symmetrically bound. In the EPR spectra of the MOP a significant amount of an additional species (HALS) was detected. Independent Mössbauer experiments[50] showed that this species is present to about 50 %. The HALS species is characteristic for axial ligation of the heme with tilted and/or twisted histidine planes. It has been postulated[39] that such a ligand environment influences the redox potential of the heme and thereby the functional properties of the protein. Different redox potentials for the two hemes in our MOP have been observed.[17, 53] This might suggest that the MOP contains two hemes with different histidine coordination geometries. The EPR/ENDOR work presented here paved the way for studies of other de novo synthesized heme proteins with less (one) or more (four) hemes, different amino acid compositions, different templates or helix linkages, and also with other cofactors. A correlation of the structural details obtained by EPR and

0947-6539/99/0508-2332 $ 17.50+.50/0 *Chem. Eur. J.* **1999**, *5*, No. 8

ENDOR spectroscopy with functional properties (e.g. redox potentials) is in progress. These studies should lead to an improved understanding and a better design of the de novo synthesized systems, such as those for electron transfer processes.

Experimental Section

Sample preparation: The synthesis of the MOP has been described.[16, 17] The incorporation of the two heme groups was basically performed as described by Choma et al.[1] except that a twofold excess of heme over the heme-binding sites was added in DMSO at once to give a maximum final concentration of 0.1 mM in 50 mM Tris/HCl (pH 8.0). The solution was stirred at room temperature for 30 min, then the unbound heme was removed by passing 1.5 mL aliquots through a Pharmacia HiTrap desalting column equilibrated with 50 mM potassium phosphate buffer (pH 7.0). The eluents containing the heme peptide were collected, desalted by a passage through a Pharmacia PD10 column and lyophilized. The lyophilized MOP sample was dissolved in 25 mM potassium phosphate buffer (pH 7.0) to reach a concentration of 730 μM (1460 μM heme). The stoichiometry of heme groups per protein molecule was determined as described in ref. [17]. The metmyoglobin–imidazole sample was obtained by adding a 250-fold excess of imidazole to a 4 mM solution of metmyoglobin. The solvent was a 2:3 mixture of glycerol and 100 mM sodium phosphate buffer (pH 7.5).
ENDOR samples containing bis-imidazole ferric heme with unlabeled and deuterated [D_4]imidazole were prepared by dissolving 16 mg (24.5 μmol) heme and 29 mg (426 μmol) imidazole or 28 mg (388 μmol) [D_4]imidazole, respectively, in 500 μL $CHCl_3$. The concentration of the bis-imidazole ferric heme complex was 49 mM with an eightfold excess of imidazole.

EPR and ENDOR measurements: X-band cw EPR spectra were recorded on a Bruker ESP 300 E spectrometer with a Bruker TE_{102} cavity equipped with a Oxford Instruments E9 helium cryostat. A temperature of about 20 K yielding optimal signal intensities was used for all EPR spectra. The microwave frequency 9.44 GHz was measured with a Hewlett Packard 5352B microwave frequency counter. The magnetic field was determined by means of a Bruker ER 035 gaussmeter. EPR spectra of a DPPH standard sample ($g = 2.0037(2)$[65]) showed that the magnetic field values are accurate within 0.1 mT at the corresponding field position of 336.6 mT.

X-band pulsed ENDOR measurements were performed on a Bruker 380E spectrometer equipped with a ESP360D-P pulsed ENDOR accessory and a Oxford Instruments CF 935 helium cryostat. The temperature for all pulsed ENDOR measurements was 5 K. The radio frequency was amplified by an ENI A 500 power amplifier. ENDOR spectra were recorded by means of a Davies pulsed ENDOR sequence.[66] The microwave π pulses were 112 ns and the microwave $\pi/2$ pulse was 56 ns long. The radiofrequency π pulse was 8 μs long and started 1 μs after the first microwave π pulse. The second microwave π pulse followed 3 μs after the end of the radiofrequency pulse. The time τ between the pulses of the detection Hahn-echo sequence was 256 ns.

Acknowledgments

This work was supported by the Volkswagen-Stiftung, program: *Intra- and intermolecular electron transfer*. Support from Fonds der Chemischen Industrie (to WL and WH) is also gratefully acknowledged.

[1] C. T. Choma, J. D. Lear, M. J. Nelson, P. L. Dutton, D. E. Robertson, W. F. DeGrado, *J. Am. Chem. Soc.* **1994**, *116*, 856–865.
[2] D. E. Robertson, R. S. Farid, C. C. Moser, J. L. Urbauer, S. E. Mulholland, R. Pidikiti, J. D. Lear, A. J. Wand, W. F. DeGrado, P. L. Dutton, *Nature* **1994**, *368*, 425–432.
[3] F. Nastri, A. Lombardi, G. Morelli, O. Maglio, G. D'Auria, C. Pedone, V. Pavone, *Chem. Eur. J.* **1997**, *3*, 340–349.
[4] S. Sakamoto, S. Sakurai, A. Ueno, H. Mihara, *Chem. Commun*. **1997**, 1221–1222.
[5] W. A. Kalsbeck, D. E. Robertson, R. K. Pandey, K. M. Smith, P. L. Dutton, D. F. Bocian, *Biochemistry* **1996**, *35*, 3429–3438.
[6] P. A. Arnold, W. R. Shelton, D. R. Benson, *J. Am. Chem. Soc*. **1997**, *119*, 3181–3182.
[7] B. R. Gibney, S. E. Mulholland, F. Rabanal, L. P. Dutton, *Proc. Natl. Acad. Sci. USA* **1996**, *93*, 15041–15046.
[8] S. E. Mulholland, B. R. Gibney, F. Rabanal, P. L. Dutton, *J. Am. Chem. Soc*. **1998**, *120*, 10296–10302.
[9] L. Regan, N. D. Clarke, *Biochemistry* **1990**, *29*, 10878–10883.
[10] T. Handel, W. F. DeGrado, *J. Am. Chem. Soc*. **1990**, *112*, 6710–6711.
[11] G. R. Dieckmann, D. K. McRorie, D. L. Tierney, L. M. Utschig, C. P. Singer, T. V. O'Halloran, J. E. Penner-Hahn, W. F. DeGrado, V. L. Pecoraro, *J. Am. Chem. Soc*. **1997**, *119*, 6195–6196.
[12] S. K. Chapman, S. Daff, A. W. Munro, *Struct. Bond*. **1997**, *88*, 39–70.
[13] B. R. Gibney, F. Rabanal, K. S. Reddy, P. L. Dutton, *Biochemistry* **1998**, *37*, 4635–4643.
[14 S. F. Betz, P. A. Liebman, W. F. DeGrado, *Biochemistry* **1997**, *36*, 2450–2458.
[15] M. Mutter, E. Altmann, K.-H. Altmann, R. Hersperger, P. Koziej, K. Nebel, G. Tuchscherer, S. Vuilleumier, H. U. Gremlich, K. Müller, *Helv. Chim. Acta* **1988**, *71*, 835–847.
[16] H. K. Rau, W. Haehnel, *Ber. Bunsenges. Phys. Chem*. **1996**, *100*, 2052–2056.
[17] H. K. Rau, W. Haehnel, *J. Am. Chem. Soc*. **1998**, *120*, 468–476.
[18] W. R. Widger, W. A. Cramer, R. G. Herrmann, A. Trebst, *Proc. Natl. Acad. Sci. USA* **1984**, *81*, 674–678.
[19] Z. Zhang, L. Huang, V. M. Shulmeister, Y.-I. Chi, K. K. Kim, L.-W. Hung, A. R. Crofts, E. A. Berry, S.-H. Kim, *Nature* **1998**, *392*, 677–684.
[20] G. Palmer in *The Porphyrins*, *Vol. IV* (Ed.: D. Dolphin), Academic Press, **1978**, pp. 313–353.
[21] C. P. S. Taylor, *Biochim. Biophys. Acta* **1977**, *491*, 137–149.
[22] R. S. Farid, D. E. Robertson, C. C. Moser, D. Pilloud, W. F. DeGrado, P. L. Dutton, *Biochem. Soc. Trans.* **1984**, *22*, 689–694.
[23] C. P. Scholes in *Multiple Electron Resonance Spectroscopy* (Eds.: M. M. Dorio, J. H. Freed), Plenum, NY, **1979**, pp. 297–329.
[24] R. B. Gennis, B. Barquera, B. Hacker, S. R. V. Doren, S. Arnaud, A. R. Crofts, E. Davidson, K. A. Gray, F. Daldal, *J. Bioenerg. Biomembr*. **1993**, *25*, 195–209.
[25] M. Mutter, S. Vuilleumier, *Angew. Chem.* **1989**, *101*, 551–571; *Angew. Chem. Int. Ed. Engl.* **1989**, *28*, 535–554.
[26] A. K. Wong, M. P. Jacobson, D. J. Winzor, D. P. Fairlie, *J. Am. Chem. Soc*. **1998**, *120*, 3836–3841.
[27] W. E. Blumberg in *Magnetic Resonance in Biological Systems* (Eds.: A. Ehrenberg, B. G. Malmström, T. Vänngård), Pergamon, **1967**, pp. 119–133.
[28] J. Peisach, W. E. Blumberg, A. Adler, *Ann. NY Acad. Sci*. **1973**, *206*, 310–327.
[29] G. Feher, R. A. Isaacson, C. P. Scholes, R. Nagel, *Ann. NY Acad. Sci*. **1973**, *222*, 86–101.
[30] C. Lionetti, M. G. Guanziroli, F. Frigerio, P. Ascenzi, M. Bolognesi, *J. Mol. Biol*. **1991**, *217*, 409–412; Brookhaven National Laboratory Protein Data Bank entry: 1MBI.
[31] H. Hori, *Biochim. Biophys. Acta* **1971**, *251*, 227–235.
[32] K. R. Carter, A. Tsai, G. Palmer, *FEBS Letters* **1981**, *132*, 243–246.
[33] W. R. Hagen, *J. Magn. Reson*. **1981**, *44*, 447–469.
[34] C. More, J. P. Gayda, P. Bertrand, *J. Magn. Reson*. **1990**, *90*, 486–499.
[35] W. R. Hagen in *Advanced EPR* (Ed.: A. J. Hoff), Elsevier, **1989**, pp. 785–813.
[36] W. R. Hagen, D. O. Hearshen, R. H. Sands, W. R. Dunham, *J. Magn. Reson.* **1985**, *61*, 220–232.
[37] M. Rivera, C. Barillas-Mury, K. A. Christensen, J. W. Little, M. A. Wells, F. A. Walker, *Biochemistry* **1992**, *31*, 12233–12240.
[38] F. S. Mathews in *The Porphyrins, Vol. VII* (Ed.: D. Dolphin), Academic Press, **1979**, pp. 108– 147.
[39] F. A. Walker, B. H. Huynh, W. R. Scheidt, S. R. Osvath, *J. Am. Chem. Soc*. **1986**, *108*, 5288–5297.
[40] G. Palmer in *Iron Porphyrins*, *Vol. II* (Eds.: A. B. P. Lever, H. B. Gray), Addison-Wesley, **1983**, pp. 45–88.
[41] S. M. Soltis, C. E. Strouse, *J. Am. Chem. Soc*. **1988**, *110*, 2824–2829.

[42] M. P. Byrn, B. A. Katz, N. L. Keder, K. R. Levan, C. J. Margurany, K. M. Miller, J. W. Pritt, C. E. Strouse, *J. Am. Chem. Soc.* **1983**, *105*, 4916 – 4922.
[43] N. V. Shokihirev, F. A. Walker, *J. Am. Chem. Soc.* **1997**, *120*, 981 – 990.
[44] R. Quinn, J. S. Valentine, M. P. Byrn, C. E. Strouse, *J. Am. Chem. Soc.* **1987**, *109*, 3301 – 3308.
[45] C. P. Scholes, K. M. Falkowski, S. Chen, J. Bank, *J. Am. Chem. Soc.* **1986**, *108*, 1660 – 1671.
[46] G. T. Babcock, W. R. Widger, W. A. Cramer, W. A. Oertling, J. G. Metz, *Biochemistry* **1985**, *24*, 3638 – 3645.
[47] J. C. Salerno, *J. Biol. Chem*. **1984**, *259*, 2331 – 2336.
[48] C. T. Migita, M. Iwaizumi, *J. Am. Chem. Soc.* **1981**, *103*, 4378 – 4381.
[49] F. A. Walker, D. Reis, V. L. Balke, *J. Am. Chem. Soc*. **1984**, *106*, 6888 – 6898.
[50] M. Reiner, F. Parak, personal communication.
[51] N. R. Orme-Johnson, R. E. Hansen, H. Beixert, *J. Biol. Chem*. **1974**, *249*, 1925 – 1939.
[52] S. Iwata, J. W. Lee, K. Okada, J. K. Lee, M. Iwata, B. Rasmussen, T. A. Link, S. Ramaswamy, B. K. Jap, *Science* **1998**, *281*, 64 – 71; Brookhaven National Laboratory Protein Data Bank entry: 1BCC.
[53] E. Katz, V. Heleg-Shabtai, I. Willner, H. K. Rau, W. Haehnel, *Angew. Chem*. **1998**, *110*, 3443 – 3447; *Angew. Chem. Int. Ed.* **1998**, *37*, 3253 – 3256.
[54] B. M. Hoffman, V. J. DeRose, P. E. Doan, R. J. Gurbiel, A. L. P. Houseman, J. Telser in *Biological Magnetic Resonance, 13* (Eds.: L. J. Berliner, J. Reuben), Plenum, **1993**, pp. 151 – 218.
[55] J. Hüttermann in *Biological Magnetic Resonance*, *13* (Eds.: L. J. Berliner, J. Reuben), Plenum, **1993**, pp. 219 – 252.
[56] Note that these values obtained at g_y are not necessarily the principal hyperfine tensor values, see ref. [57].
[57] G. C. Hurst, T. Henderson, R. W. Kreilick, *J. Am. Chem. Soc*. **1985**, *107*, 7294 – 7299.
[58] D. M. Collins, R. Countryman, J. J. Hoard, *J. Am. Chem. Soc*. **1972**, *94*, 2066 – 2072.
[59] D. K. Geiger, Y. J. Lee, W. R. Scheidt, *J. Am. Chem. Soc*. **1984**, *106*, 6339 – 6343.
[60] These values were calculated assuming a C–H bond length of 1.1 Å and standard geometry.
[61] L. Banci, I. Bertini, H. B. Gray, C. Luchinat, T. Reddig, A. Rosato, P. Turano, *Biochemistry* **1997**, *36*, 9867 – 9877.
[62] S. D. Emerson, G. N. La Mar, *Biochemistry* **1990**, *29*, 1556 – 1566.
[63] J. D. Satterlee, G. N. La Mar, *J. Am. Chem. Soc*. **1976**, *98*, 2804 – 2808.
[64] G. N. La Mar, J. S. Frye, J. D. Satterlee, *Biochim. Biophys. Acta* **1976**, *428*, 78 – 90.
[65] J. A. Weil, J. R. Bolton, J. E. Wertz in *Electron Paramagnetic Resonance*, John Wiley, New York, **1994**, p. 511.
[66] E. R. Davies, *Phys. Lett*. A **1974**, *47*, 1 – 2.
[67] T. E. Creighton in *Proteins: Structure and Molecular Properties*, W. H. Freeman, New York, **1993**, p. 13.

Received: December 4, 1998 [F1478]

  0947-6539/99/0508-2334 $ 17.50+.50/0